SLAC-PUB-10907
December 2004

Automated Electric Charge Measurements of Fluid Microdrops Using the Millikan Method*

Eric R. Lee, Valerie Halyo, Irwin T Lee, Martin L. Perl

Stanford Linear Accelerator Center

2575 Sand Hill Road

Menlo Park, CA 94025

Abstract

Automated measurements of the electric charge of fluid microdrops precise to up to 0.016 of an electron charge have been made using machine-vision systems to observe the motion of fluid microdrops in air under the influence of an oscillating electric field. The fluid drop diameters have ranged from 7 to 25 μm with smaller diameter drops being measured to higher precision. The experimental runs performed for the purpose of attempting to find isolated fractionally electrically charged particles have measured the charges of tens of millions of fluid microdrops using piezoelectrically driven drop-on-demand inkjet-like droplet ejectors as fluid drop sources.

1. Introduction

The quantization of free electric charge into units only of multiples of the unit charge on the electron and not into any smaller sub-fraction is an issue that is the subject historically of many experimental tests. One method of searching for isolated fractional electric charge has been to expand upon the method used by Robert Millikan to perform the original determination of the value of the fundamental unit charge by measuring the electric charges of fluid microdrops based on their terminal velocities in a switched electric field. The incorporation of machine-vision systems based on commercial grade CCD cameras coupled to personal computers, using microdrop generators based on inkjet printing technology has allowed automation of Millikan's method using relatively low-cost hardware. The charge-measurement accuracy of these systems can be made limited only by the Brownian motion of the fluid microdrops.

2. Measurement physics

The principle behind the Millikan method of determining the electric charge on a fluid microdrop of known specific gravity is to measure the terminal velocity of the microdrops under the influence of electric fields in a well-characterized gas environment and extract from these

* This work was supported by Department of Energy contract DE-AC02-76SF00515.

Published in Metrologia 41:S147-S158,2004

terminal velocity measurements the radius and the electric charge of the microdrops [1,2]. The following quantities are used in this paper:

F = force
ρ = fluid density
m = microdrop mass
g = gravitational acceleration
v = drop velocity relative to air
r = drop radius
η = viscosity of air
E = electric field
Q = charge on microdrop
T = temperature
k = Boltzmann's constant
t = time in seconds
$N_e = Q/e$ number of electron charges

2.1 Stokes' Law

The charge on fluid microdrops, using Millikan's method, is determined by measuring the terminal velocity of the drop in a known electric field. The drop is accelerated by the electric field and reaches terminal velocity when the forces, due to gravity (1) and its electric charge (2), equal the counterforce from frictional forces due to air resistance (3). At the low Reynolds' numbers that characterize fluid microdrops at terminal velocity the air resistance is determined to a high degree of accuracy by Stokes' Law with the Cunningham correction factor added in for measurements involving very small drops:

$$F_{\text{Gravity}} = mg \tag{1}$$

$$F_{\text{Electric}} = QE \tag{2}$$

$$F_{\text{Stokes}} = 6\pi\eta r v. \tag{3}$$

The Cunningham correction factor is a correction to Stokes' Law to account for the fact that the atmosphere is not a perfect continuum. The net result is that the resistance of the air is slightly less than that predicted by Stokes' Law. The error is about 16% for 1 μm diameter drops and falls to a correction of less than 2% for 10 μm diameter drops. A modern form for $C_{\text{Cunningham}}$ is:

$$F_{\text{Stokes}} = 6\pi\eta r v / C_{\text{Cunningham}}$$

$$C_{\text{Cunningham}} = 1 + (\lambda/r)\,(A + B\exp[-br/\lambda]) \tag{4}$$

where r is the drop radius. Typical values for Cunningham correction variables for air at standard temperatures and pressure are [3]

$$A = 1.252$$
$$B = 0.399$$
$$b = 1.100$$

λ = 0.065 μm (mean free path of the gas molecules)

2.2 Relaxation time constant

Equation (5) gives the relaxation time constant for coming to terminal velocity after a change in the forces exerted on the microdrop. For drops of the diameter typically measured in automated Millikan apparatus (7 - 25 μm in diameter) the relaxation time constant is of the order of a millisecond or less. This is generally much smaller than the electrical switching time constants associated with the precision switching of high voltages to the electric-field plates, resulting in the drops being at continual terminal-velocity equilibrium with changes in the electric field:

$$\tau = (2/9)\ (\rho r^2/\eta) \quad \text{relaxation time constant.} \tag{5}$$

2.3 Charge determination

For a Millikan experiment with electric fields oriented parallel to the direction of fall due to gravity, the forces on the drop due to the electric field are summed with that of gravity and then balanced against the fluid dynamic resistance to motion due to Stokes' Law, to obtain net terminal velocities for the microdrops for two different values of the applied electric field (figure 1). For maximum measurement accuracy the values of the applied electric field are the maximum magnitudes sustainable without gas-media breakdown, applied in opposite directions (E_{up}, E_{down}) for equal time intervals. This will produce a time-average downward microdrop terminal velocity equal to that of gravity acting alone (8).

$$mg + QE_{\text{down}} = 6\pi\eta r v_{E\text{down}} \quad \text{Forces on a microdrop with the electric field oriented with gravity} \tag{6}$$

$$mg - QE_{\text{up}} = 6\pi\eta r v_{E\text{up}} \quad \text{Forces on a microdrop with the electric field oriented opposing gravity} \tag{7}$$

$$v_g = (1/2)\ (v_{E\text{down}} + v_{E\text{up}}) \quad \text{Net average downward velocity imparted to a microdrop by gravity.} \tag{8}$$

Using (1), (2), and (3), the charge (9) and radius (10) of the fluid microdrop can be calculated by measuring only the fluid drop's terminal velocity in two different electric fields:

$$N_e = (9\pi/e)[2/[(\rho_{\text{fluid}} - \rho_{\text{air}})g]]^{1/2}\ \eta^{3/2}[(v_{E\text{down}} - v_{E\text{up}})/(E_{\text{down}} + E_{\text{up}})]\ [(v_{E\text{up}}E_{\text{down}} + v_{E\text{down}}E_{\text{up}})/(E_{\text{up}} + E_{\text{down}})]^{1/2} \tag{9}$$

$$r = 3(\eta/[(\rho_{\text{fluid}} - \rho_{\text{air}})2g])^{1/2}\ [(v_{E\text{up}}E_{\text{down}} + v_{E\text{down}}E_{\text{up}})/(E_{\text{up}} + E_{\text{down}})]^{1/2}\ . \tag{10}$$

2.4 Horizontal electric field

For a Millikan apparatus where the electric field is oriented perpendicular to gravity (figure 2), the radius of the microdrop is determined by measuring the vertical terminal velocity component, taking into account the optional use of laminar airflow to slow the fall of the drop. Given a known radius from the vertical terminal velocity measurement, the charge of the drop can be calculated from the lateral terminal velocity and the value of the electric field [6,7,8]:

$v_{vertical} = (2/9)\,[(\rho_{fluid} - \rho_{air})r^2 g/\eta]$ Vertical terminal velocity component due to gravity (11)

$v_{lateral} = QE/6\pi\eta r$ Lateral terminal velocity due to electrical forces (12)

$r = 3\,[(\eta v_{vertical})/(\rho_{fluid} - \rho_{air})2g]^{1/2}$ Radius of a microdrop from its measured vertical terminal velocity (13)

$N_e = (1/e)\,[v_{vertical}/((\rho_{fluid} - \rho_{air})2g)]^{1/2}\ \eta^{3/2}\,(18\pi v_{lateral}/E)$ Charge on a microdrop from its measured horizontal terminal velocity. (14)

2.4.1 Air flow reduction of vertical terminal velocity

The electrode geometry of a Millikan experiment with horizontal electric field allows for the use of regulated laminar airflow to reduce the vertical terminal velocity of falling microdrops. This can make possible the accurate charge measurement of large diameter microdrops that under free fall in still air would have terminal velocities too large to take multiple velocity measurements in the limited field of view of the machine-vision imaging systems when set at optimal magnifications for precision centroiding [8, 9].

The velocity profile of laminar airflow in a duct is a solved problem and is given by [10]

$$V_{air}(x, y) = 1 - x^2/b^2 + 32/\pi^3 \sum_{n=1,3,5,..}^{\infty} (-1)n^{-3}2^{n-1} \times \cosh(n\pi y/2b)\cos(n\pi x/2b)/\cosh(n\pi a/2b) \quad (15)$$

where a is the half-width of the air duct in the long direction, b the half-width of the air duct in the short direction, x the distance from the duct center axis in the short direction and y is the distance from the duct centre axis in the long dimension (figure 3).

3. Measurement error sources

Measurement error in the charge of the microdrops can arise both from sources that can be minimized through proper engineering, and from causes that are intrinsic to the physics of the Millikan method.

3.1 Brownian motion

Since the physics of this experiment relies upon the use of Stokes' Law to provide a force proportional to the velocity of the drop and its radius, the gas molecules, in addition to furnishing a frictional counterforce to gravity and the electric forces, also introduce a source of measurement error arising from Brownian motion. This is the major irreducible source of measurement error in Millikan-type charge-measurement apparatus.

The Brownian error in a terminal velocity measurement is given by

$$\sigma_{VBrownian} = [kT/3\pi\eta r\Delta t]^{1/2} \quad (16)$$

where Δt is the measurement interval.

3.1.1 Horizontal electric field

For a Millikan-type charge-measurement apparatus with horizontally oriented electric fields the charge on the microdrop can be expressed as

$$Q = (9\pi/E)\,[2/\rho g]^{1/2}\,\eta^{3/2}\,[v_{\text{vertical}}]^{1/2} v_{\text{lateral}}. \tag{17}$$

Grouping together in the constant C the terms that are not varied by Brownian motion:

$$C = (9\pi/E)\,[2/\rho g]^{1/2}\,\eta^{3/2}.$$

The equation for the determination of drop charge can be rewritten in simplified form as

$$Q = C\, v_{\text{vertical}}{}^{1/2} v_{\text{lateral}}. \tag{18}$$

Measurement error arising from Brownian motion enter as

$$\sigma_Q = C\sigma_{\text{Brownian}}\,[(v^2_{\text{lateral}}/4v_{\text{vertical}}) + v_{\text{vertical}}]^{1/2} \tag{19}$$

with the fractional error in Q being expressed as

$$\sigma_Q/Q = \sigma_{\text{Brownian}}\,[(1/4v^2_{\text{vertical}}) + (1/v^2_{\text{lateral}})]^{1/2}. \tag{20}$$

3.1.2 Vertical electric field

In a Millikan apparatus with a vertically oriented electric field, the magnitudes of the two values of the electric field used are

$$E_{\text{up}} = -E_{\text{down}}.$$

The equation for the charge of the microdrop as a function of the measured terminal velocities can be derived from equation (9) and expressed as

$$Q = (9\pi/E)[2/\rho g]^{1/2}\ \eta^{3/2}[v_{E\text{down}} + v_{E\text{up}}]^{1/2}(v_{E\text{down}} - v_{E\text{up}}). \tag{21}$$

By noting that in a Millikan device with symmetrically switched vertical electric field the average of the two measured terminal velocities is equal to that of the terminal velocity due to gravity and fluid dynamic friction alone, v_g, and that half the difference in the terminal velocities gives a term equivalent to the v_{lateral} term from the horizontal electric field orientation:

$$V_g = (v_{E\text{down}} + v_{E\text{up}})/2\ , \qquad v_E = (v_{E\text{down}} - v_{E\text{up}})/2\ .$$

Using these substitutions, an equation for the charge of a fluid microdrop in a vertical electric field very similar in form to that for the charge of a fluid microdrop in a Millikan apparatus with horizontal electric field can be written as

$$Q = C\, v_g{}^{1/2} v_E. \tag{22}$$

The equation for charge-measurement error with a vertically applied electric field due to Brownian motion, while identical in form to that for the horizontal electric field case, differs by a

factor of the square root of two due to an additional implicit doubling of the measurement interval taken in order to obtain two terminal velocity measurements:

$$\sigma_Q = C\sigma_{\text{Brownian}}(2^{-1/2})\,[(v^2{}_E/(4v_g) + v_E]^{1/2}. \qquad (23)$$

Similarly, since the Brownian-motion error is random, one can, in principle, reduce this source of error regardless of the electric field configuration by taking multiple measurements of the same drop, which for N independent measurements will reduce the error by a factor $N^{-1/2}$.

3.2 Charge magnitude

An analysis of the error on charge measurement in a Millikan apparatus shows that given a fixed error in terminal velocity measurement due to Brownian motion, the widths of the charge-measurement distributions around the integer charge values increase as the absolute magnitude of the charge on the drops increases. This reduces the sensitivity of experiments intended to detect fractionally charged matter or measure the value of e when the magnitude of the charges of the drops one is using is large. This increased measurement error is due to the uncertainty in the microdrop radius propagating into the charge-measurement error as a factor that increases with charge magnitude. Intuitively, the charge on a drop is determined by dividing the magnitude of the measured displacement under a known electric field by the radius of the drop (modulo physical constants). The uncertainty in the radius, thus, has a larger contribution when the displacement and, hence, the charge are large.

Generalizing equation (19) for the error due to Brownian motion on charge for a Millikan apparatus with horizontal electric field, one can obtain an expression from which one can derive the effect of the magnitude of the charge on the fluid drop on the accuracy to which this charge can be measured:

$$\sigma_Q = C\,[(v^2{}_{\text{lateral}}/4v_{\text{vertical}})\;\sigma^2{}_{\text{vertical}} + v_{\text{vertical}}\sigma^2{}_{\text{lateral}}]^{1/2}. \qquad (24)$$

Since v_{lateral} is proportional to drop charge, the error in measured charge increases with the magnitude of the charge on the fluid drop.

Using the variable substitutions and simplifying assumptions concerning the electric fields of section 3.1.2,

$E_{\text{up}} = -E_{\text{down}}$, $\quad V_g = (v_{E\text{down}} + v_{E\text{up}})/2$, $\quad v_E = (v_{E\text{down}} - v_{E\text{up}})/2$,

equation (25) can be derived for the charge-measurement error in a Millikan apparatus with vertical electric field, which, like equation (24), also shows an increase in drop-measurement error with increases in the magnitude of the charges measured since the v_E which corresponds to the v_{lateral} term, also scales linearly with charge:

$$\sigma_Q = (C/2)\,[(v_E/(2v_g{}^{1/2}) + v_g{}^{1/2})^2\,\sigma^2 v_{\text{down}} + (v_E/(2v_g{}^{1/2}) - v_g{}^{1/2})^2\;\sigma^2 v_{\text{up}}]^{1/2}. \qquad (25)$$

If the uncertainties in the measurements of the terminal velocities for the upward and downward phases of the electric field are the same

$$\sigma_v = \sigma_{V\text{up}} = \sigma_{V\text{down}}$$

then equation (25) can be simplified into a form identical to that of equation (23), which defines the uncertainty in the charge measurement for a Millikan apparatus with horizontal electric field.

$$\sigma_Q = C2^{-1/2}\sigma_v [(v^2_E/4v_g) + v_E]^{1/2}. \quad (26)$$

3.3 Diameter

In the equations for the error in fluid-drop charge, (24) and (25), there is a drop diameter dependence in the v_g (vertical terminal velocity) term, as well as a measurement-uncertainty-error term exclusively due to Brownian motion. Since the increase of error with increasing drop diameter dependent on terminal velocity enters as a higher polynomial power than the decrease in error with increasing drop diameter dependent on Brownian motion error, the total charge-measurement error increases as the drop diameter increases. The increase in terminal velocity with diameter also decreases measured accuracy in practical systems due to the drop remaining in the field of view a shorter amount of time, reducing the number of independent measurements it is possible to take. As examples of the practical accuracy it is possible to achieve as a function of microdrop diameter, our experimental apparatus has achieved 1/60*e* accuracy for 7.6 μm diameter drops, and 1/30*e* charge measurement accuracy for 20 μm diameter drops.

3.4 Charge changes during measurement

Microdrops are capable of experiencing charge changes during a terminal velocity measurement due to collisions with atmospheric ions or from cosmic rays. This can give the appearance of a fractional electric charge. The only way of guarding against this source of error is by designing the apparatus such that multiple independent charge measurements can be taken of each fluid drop along with a consistency check used to ensure that the charge on the drop has not changed while being measured. In practice, this is a rare occurrence with the highest level of these events referenced in an automated Millikan experiment being given as one suspected charge change per thousand drops measured [11].

3.5 Temperature

Temperature enters into the measurement error primarily as it varies gas viscosity. Secondary effects are variable buoyancy related to the density of the air relative to the fluid, and the variance in the magnitude of the Brownian motion error.

A common empirical expression for the variation of gas viscosity with temperature is the Sutherland equation [12]:

$$\eta = (aT^{3/2})/(b + T). \quad (27)$$

The constants a and b for air are $a = 1.485 \times 10^{-6}$ kg m^{-1} s^{-1} K$^{-1/2}$ and $b = 110.4$ K.

The density of air ρ_{air} has a temperature dependence given by

$$\rho_{air} = CP/T \quad (28)$$

where $C = 3.489 \times 10^{-3}$ kg K/ m^3 Pa^{-1}.

As an example, for the vertical electric field case, the equation for the extraction of the charge (29) of the drop from its terminal velocity can be rewritten in its temperature-dependent form (30), taking into account the variation in buoyancy and viscosity with temperature:

$$N_e = (9\pi/e)[2/[(\rho_{fluid} - \rho_{air})g]]^{1/2}\, \eta^{3/2}[(v_{Edown} - v_{Eup})/(E_{down} + E_{up})] \times [(v_{Eup}E_{down} + v_{Edown}E_{up})/(E_{up} + E_{down})]^{1/2} \quad (29)$$

$$N_e = (9\pi/e)[2/[(\rho_{fluid} - (CP/T)_{air})g]]^{1/2}[(aT^{3/2})/(b + T)]^{3/2} + [(v_{Edown} - v_{Eup})/(E_{down} + E_{up})]\,[(v_{Eup} + E_{down} + v_{Edown}E_{up})/(E_{up} + E_{down})]^{1/2}. \quad (30)$$

Since the measurement chambers were monitored to a resolution of 0.1 K with electronic thermometry devices while being maintained isothermal to better than tenths of a kelvin, temperature variation as a source of measurement error was a small effect compared with the error due to Brownian motion. As an example, for 7 μm diameter fluid drops falling in air at standard temperature and pressure an uncompensated error of 2.5 K translated to an error in calculated drop charge of less than 0.01*e*.

4. Measurement optimization

The analysis in sections 3.1-3.5 suggests how an automated Millikan apparatus should be designed for maximum charge-measurement accuracy.

4.1 Electric field

The electric-field magnitude should be the maximum value that does not initiate gas breakdown to maximize the spatial displacement per unit charge per unit time. The field gradients in the measurement zone should be minimized in order that induced dipole forces do not become significant sources of error. The switched electric field waveform should be in the form of a symmetric square wave.

4.2 Magnification

There is a minimum magnification needed to centroid the microdrops to an accuracy at which Brownian motion becomes the limiting factor in charge measurement. Above this threshold charge-measurement accuracy does not increase. The magnification needed is that which projects the image of the microdrop over several pixels so that subpixel position determinations can be achieved; with sufficient contrast the centroiding error due to imaging-chip-pixel noise is not significant.

4.3 Droplet spacing

The motion of charged microdrops in an oscillating electric field can be coupled by fluid dynamic effects to other nearby microdrops. This can produce very strong charge-measurement artifacts. In principle, two adjacent drops with different electric charges but identical diameters falling proximal to each other can have consistently offset-measured electric charges. Measurements performed with 20 μm diameter drops required an interdrop spacing of 600 μm or more for the measurement error caused by the interdrop fluid dynamic interactions to fall below that of the Brownian error—the wider the interval between adjacent, introduced microdrops, the smaller this effect.

A widely separated ensemble of drops falling together having different electric charges can produce two other sources of error. If the drops, as a unit, do not have an average charge of zero, then a small average offset can be observed in the measured charges of each individual drop as the air volume, as a whole, is given a non-zero average net motion during each electric-field polarity switching. In addition, a spatially dense stream of microdrops falling under gravity can produce a streaming effect as the air along the average trajectory of the fluid drops is set into net motion. These effects are minimized by keeping the drop density per unit air volume low [13][14].

4.4 Droplet diameter

Smaller drops given, their greater displacement per unit charge. are measured with higher accuracy than larger drops. Mass throughput is lower though, and in practice it is more difficult to operate and maintain fluid microdrop ejectors as the diameters of the microdrops that they are required to generate are reduced in size because the increase in the number of stray particles that are capable of clogging the nozzle increases as the diameter of the nozzle is made smaller.

As drops increase in diameter, secondary measurement artifacts that scale with the cube of the drop diameter such as induced dipole and electric-field gradient-induced forces start to become sources of error. The relaxation time constant for drops to come to terminal velocity after changes in the electric field starts to become a significant part of the electric field interval (~0.1 s) at each polarity at diameters larger than 50 μm.

Since the drops have an average downwards motion due to gravity, large drops will have a shorter dwell time in the camera's field of view, providing poorer measurement statistics.

5. Measurement apparatus

5.1 Design factors

5.1.1 Mechanical

The positional measurement accuracy required to perform charge measurements on is on the order of a micrometer or less on the centroided positions of the fluid microdrops. This requires that the measurement region be a controlled environment free from convection and vibration. Some microdrop charge measurement experiments surrounded the measurement chamber with temperature-regulated fluid in order to eliminate temperature-gradient-induced convection. Fluid immersion, while effective, makes maintenance inconvenient and time consuming. Our experiments found that placing the measurement chamber within two concentric enclosures (a 'box in a box') was effective enough to control thermal convection. The design of the convective shielding enclosures was a metal frame with transparent polycarbonate walls with optical windows installed where the imaging system views the microdrops.

Vibrational control was implemented by mounting the drop-measurement chamber and the optical imaging system rigidly on a vibrationally damped optical table. The rigidity of the apparatus was tested by imaging a static test target mounted in the measurement chamber. The relative motion due to vibration of the measurement chamber and optical components was found to be negligible.

Vibration can also cause measurement errors due to relative motion between the apparatus and microdrops as they are in free fall. Spectral measurements of the vibrations present showed that most of the amplitude was in the low-frequency range, below 100 Hz. Since the apparatus is small compared to the wavelength of sound at these frequencies, the air enclosed in the system can be considered to move with the apparatus. Since the time constant for fluid microdrops to reach terminal velocity is on the order of a millisecond, at frequencies much less than 1 kHz, the approximation that the microdrops move rigidly with the air is a good one. This reduces greatly the effect of vibration on the actual measurement process.

5.1.2 Electric field

Since the displacement of a charged microdrop is dependent on the charge of the microdrop and the time integral of the electric field that it experiences, it is necessary to have a well-characterized electric field in the measurement zone. While, in principle, a non-constant electric field environment can be modeled and used for charge measurements, there are other factors, in addition to calculational simplicity, that make uniform electric fields desirable. The displacement per unit charge per unit time is used to determine the value of the electric charge in a Millikan apparatus. Given a constant positional measurement uncertainty one would want to maximize this differential spatial displacement for differential values of charge displacement by using the highest electric-field magnitude possible. This is usually limited by high-voltage gas breakdown. Since the time-integrated displacement of a droplet with a given charge is maximized by operating at an electric-field magnitude that is at all points at a maximum value that does not initiate gas breakdown, a uniform electric field at the maximum value that does not cause corona discharge or arcing is optimal. Another practical factor is that electric-field gradients act to displace and scatter the trajectories of microdrops, amplifying any small deviations from the average injected microdrop trajectory. Modeling of the electric field electrodes was performed using Poisson software from Los Alamos National Laboratory. This software was used to determine the necessary dimensions of the electric field plates and the extent of the region where a sufficiently uniform electric field existed that accurate trajectory determinations could be made. One result of this modeling is a numerical confirmation of the empirical observation that the hole in the electric field plate through which droplets are introduced into the measurement region in a conventional Millikan experiment must be very small compared with the interplate spacing to avoid introducing significant electric field gradients. The high electric fields cause an induced dipole moment on the fluid drops, which in an electric-field gradient can cause spurious forces on the drop.

The optimal electric fields to use to maximize the charge signal from the droplet displacements were to alternate positive and negative constant-amplitude electric fields with the field magnitudes being just below the gas breakdown field strength. In these experiments the electronic configuration adopted was a single grounded electric field plate placed opposite a powered plate that alternated between potentials of $\pm$ 15 kV. Reliable high-speed switching of tens of kilovolts multiple times per second is not a simple task. It was implemented in this experiment by the use of two precision fixed high-voltage power supplies set at the desired positive and negative voltage values that were switched onto the powered electric field plate with an optically isolated vacuum-tube switch powered by a high-voltage, low-interwinding capacitance line transformer.

Some fluid-drop and dust electric charge-measurement systems have been constructed with the electric field oriented in the horizontal direction [4,5,6]. This facilitates measurements of large numbers of droplets, or dust particles, simultaneously since the droplets are not constrained to have to enter through a small area opening in the plate, as would be the case for a vertical electric field orientation. Horizontally oriented electric field plates also facilitate the use of controlled laminar airflow to slow the fall rate of large droplets facilitating their accurate charge measurement. Also, in principle, by using a horizontal electric field a crude charge and radius measurement can be taken of a fluid microdrop without the electric field having to assume multiple values, though for optimal accuracy a symmetrically oscillating electric field will yield significantly smaller charge-measurement errors. This is because under a symmetrically oscillating electric field, all drops will have the same average, downward trajectory regardless of charge, facilitating keeping the drops in the imaging field to obtain multiple, independent measurements.

5.1.3 Imaging

The microdrops are imaged by providing a stroboscopically illuminated, bright, uniformly lit background and viewing the microdrop as a dark shadow against this bright background. It was found to be easier to provide a uniform, bright background by the use of a ground-glass screen and illumination diffusers than to try to provide a uniform bright illuminated source to view the microdrop as a bright object against a uniformly dark background.

The pixel dimensions of current CCD imagers are on the order of 10 μm. The dimensions of the microdrops are also on the order of 10 μm. Since the positional accuracy required for charge extraction of droplets of these dimensions is on the order of a micrometre or less some magnification of the image plane is needed. It is desirable to use the minimum magnification necessary in order to have a wide a field as possible so that as many independent positional measurements of a microdrop be taken as possible to optimize measurement statistics. This magnification both maps the real space region where the drop travels to a larger number of pixels and increases the size and the contrast of the droplet image so that it can be centroided to subpixel resolution more accurately. For the imagers used for the series of experiments done at SLAC from 1994 to 2003, which have utilized CCD chips having pixel dimensions of 8.5 μm by 19.5 μm, the minimum magnification needed was two for drops in the 20 μm diameter range and four for droplets smaller than 10 μm. Increasing the magnification past this threshold point for a given drop diameter did not increase measurement accuracy. Since the drops are in constant motion, stroboscopic imaging is used to provide sharp images for machine-vision centroiding and for precise timing references so that velocities can be accurately determined. Early experiments utilized gas discharge strobes that have now been made obsolete by LED arrays. Both analog and digital output cameras and image acquisition cards were used for the computer with no difference found in our experiments between the two electronic readout systems.

Selection of the cameras used for these experiments was governed by the requirements that the camera have as large an imaging array as is possible while being able to read out frames fast enough for the computer to analyze the video input at a rate of 10 frames per second or faster. It was also desirable to be able to set the operation for linear response to illumination and to disable any automatic, internal gain settings since optimal, bright-background drop imaging involves average levels of illumination that would not be consistent with normally intended uses of CCD

imagers. The cameras used in these experiments were Cohu model 4110 and Cohu model 6310 cameras; both using the same imaging chip, having 755 by 242 pixels of dimension 8.5 μm by 19.5 μm, with total dimensions of 6.4 by 4.8 mm. These cameras, intended for industrial, machine-vision applications, have externally accessible frame-timing outputs. The camera's internal frame timing is controlled by crystal oscillators. This frequency stability of the camera's internal electronics allows the use of the camera's externally accessible frame synchronization outputs to be used to trigger the illumination strobes ensuring that the optical strobe outputs will always be synchronized properly to the camera image acquisition and readout cycle.

In order to reduce systematic effects due to illumination, gradients in the background illumination were minimized using a combination of multiple diffuse sources and a ground-glass screen. In addition, the remaining systematic variations were calibrated out by subtraction from the raw image data.

Several options for centroiding algorithms were evaluated, with performance (and computational time) increasing with increasing complexity. These algorithms included variations on a center-of-mass calculation, best fit based on Gaussian models, and best fit based on models incorporating a point spread function.

For the magnification and pixel density used, the typical image of a 20 μm diameter drop consisted of 50 pixels (5 pixels by 10 pixels) significantly above (3 sigma) the noise threshold. Under these conditions, the best fit algorithms were capable of positional accuracy of 1/30 of a pixel (0.31 μm in real space) [8,9].

5.1.4 Microdrop generators

Millikan generated the microdrops he used for determining the value of the electric charge by using a spray atomizer and selecting out, from the mist of droplets generated, those which by chance had fallen within the observation region of his apparatus and had appropriate diameters. The use of inkjet-like drop-on-demand fluid microdrop ejectors allows modern researchers to generate fluid microdrops on demand with a precise, pre-selected diameter and trajectory. The microdrop generators used at SLAC were based on a design invented by Zoltan in 1972 [17]. These microdrop ejectors are constructed from glass tubes having a fluid nozzle at one end with an opening approximately the diameter of the drop one wishes to generate. A piezoelectric actuator compresses the tube and ejects a short-duration fluid jet that forms into a fluid microdrop.

5.1.5 Fluids

The fluids used in automated Millikan experiments are restricted in that they must not have so high a vapor pressure that they evaporate and, in addition, the fluids must have viscosity and surface tension that allows them to be jetted from drop-on-demand microdrop generators. Dow Corning 200 silicone oil and light mineral oil of 5 cSt viscosity were the fluids used for the SLAC experiments. Current work is being done at SLAC on measuring the charges of light mineral oil containing a suspension of powdered carbonaceous chondrite meteorite. The research group at San Francisco State University has successfully used mercury and sea water as microdrop fluids for their automated Millikan apparatus [11,18,19].

5.2 Hardware implementation (table 1)

Experiment	Drops (Dia. material)	Throughput	Accuracy	Technology
Millikan (1910) [1,2]	3.4-4.7 μm (refined watch oil)	~100-200 drops 1 ng	~0.03*e*	Human observation and timing
SLAC (1994-1995) [15]	7 μm (5 cSt silicone oil)	6 million drops 1 mg	0.025*e*	Machine vision, single small diameter drop per frame
SLAC (1996-1999) [13]	7-10 μm (5 cSt silicone oil)	40 million drops 17 mg	0.02*e*	Machine vision, multiple small diameter drops per frame
SLAC (1999-2001) [8]	20 μm (5 cSt silicone oil)	17 million drops 70 mg	0.02*e*	Machine vision, horizontal electric field with laminar air flow to allow measuring large diameter drops

Table 1. Summary of automated machine vision based Millikan devices constructed and operated at Stanford Linear Accelerator Center between 1994 and 2002. Accuracy is defined as the standard deviation of the average widths of the charge peaks. Data from Robert Millikan's original experiment is listed to provide a historical reference.

Different automated variations of the standard Millikan apparatus have been constructed at SLAC for the precise high-mass throughput measurement of fluid microdrops for a sequence of experiments attempting to detect fractionally charged free particles.

The initial apparatus constructed at SLAC (1994-1995) shown in figures 4 and 5 was a prototype intended to explore whether an automated Millikan device based on video camera machine vision was feasible [15, 16]. The apparatus operated continuously over a period of a year during which the charges of 6 million microdrops charges were measured. Due to the image processing speed limits of the 66 MHz, 486-based personal computer used for real-time image analysis, the apparatus was only capable of measuring the charge of a single microdrop at a time per sequence of image frames. The limiting factor in the accuracy of the charge measurement possible was a combination of Brownian motion and the limited number of measurements possible as the microdrop passes through the 1.6 mm vertical extent of the image system's field of view.

The SLAC 1996-1999 Millikan apparatus was an attempt to increase measurement-mass throughput by measuring the electric charges of multiple microdrops simultaneously [13, 14]. The measurement of multiple drops simultaneously was facilitated by the use of more powerful computers (200 MHz Pentium II) and a modification of the drop generator system to facilitate the ejection of two-dimensional arrays of microdrops with spacings that can be arbitrarily varied. The tracking algorithms, mechanical and optical engineering were also improved based on experience with the first experiment, leading to an increase in charge-measurement accuracy despite the slightly larger average drop diameters. The limit to the increase in throughput by placing multiple drops simultaneously in the same video frame was that fluid dynamic coupling

between drops with too close a spacing alters their terminal velocities sufficiently to prevent accurate charge determination.

The SLAC (1999-2001) Millikan apparatus was an attempt to increase the mass throughput by constructing a system that facilitates the measurement of larger diameter drops than the first two SLAC systems [8,9]. This large drop Millikan apparatus utilizes a horizontally oriented electric field that allows for the use of upwards-directed, regulated laminar airflow to slow the vertical terminal velocity of the microdrops. This apparatus was capable of measuring the charges of multiple drops in the same field of view but in practice the throughput was limited by the requirement that drops be spaced far enough apart that fluid dynamic coupling between adjacent drops not affect their independent terminal velocities.

6. Future improvements

6.1. Machine vision

The automated Millikan-charge-measurement apparatus was made possible by modern machine-vision technology, powerful low-cost computers, and inexpensive large scale data storage. The capabilities of machine-vision camera and image processing software over time are expected to continue to increase in the near future which will translate by different quantitative factors into higher mass throughput and increased accuracy. Increases in the sizes and resolution of the camera field that the machine-vision system can process in real time linearly scale up the mass throughput by allowing the simultaneously imaging and measurement of more fluid drops. Increases in the real-space field of view will also increase charge-measurement accuracy by the square root of the increase in the linear extent of the field of view due to the increase in measured points. When it becomes possible to model and compute the drop-to-drop fluid dynamic interactions in real time and remove this source of charge-measurement error, the mass throughput will increase as the square of the factor of reduction in the currently required minimum interdrop spacing.

6.2 Network computing

The incorporation of other recent technologies such as reliable, low-cost, high-speed date networking is extending the capabilities of the experimental system. An automated Millikan system that has just complete the initial test run at SLAC (2004) utilizes multiple cameras and multiple networked computers operating together in real time to allow the high mass throughput charge measurement of fluid containing suspensions of exotic test materials such as meteorite dust, where the characteristics of the fluids and the drops change over short periods of time, which necessitates active feedback control over multiple aspects of the charge-measurement system and drop generation hardware.

6.3. Increased drop size

The larger the drops one can effectively measure, the higher the mass throughput per unit time. The principal limiting factor in measuring the charges of large drops using the Millikan method is that as the size of the drops increases, the terminal velocity increases, ultimately limiting the number of position measurements it is possible to make, thus limiting the accuracy of the charge determination. As implied in section 6.1, imaging systems with larger real-space fields of view will allow the measurement of larger drops with the same charge-measurement error. We have

demonstrated that vertical regulated laminar airflow can be used to slow the fall rate of large diameter fluid drops sufficiently to allow accurate measurements to be made of fluid drops up to 27 μm in diameter; however, the spatially non-uniform nature of the laminar airflow significantly complicates the generation of evenly spaced, spatially dense arrays of simultaneously measured microdrops. The best solution to this problem of how to optimally operate a Millikan apparatus to allow the accurate high mass throughput measurement of large diameter fluid drops may have to wait until future generations of experimentalists are able to set up and operate Millikan systems in significantly lower gravitational fields.

7. Scientific status of fractional charge searches

Before concluding this paper we provide some references to other methods of searching for fractionally charged elementary particles and to the more recent results of these searches. There are three general ways to search for fractionally charged elementary particles: searches in bulk matter [20] such as the Millikan technique described in this paper, searches using particle accelerators and colliders, and searches in cosmic rays or in other particle flux impinging on the Earth.

Unfortunately, there is no recent review paper devoted solely to searches for fractionally charged particles. The most recent review of such searches is part of a more general review paper on searches for stable, massive elementary particles [21].

There are two main ways to search for fractionally charged particles in bulk matter—the Millikan drop method and the levitometer method [20,22,23]. The Millikan method has been used with sea water [19], mercury [11], and by us with silicone oil [8,13,15]. The levitometer method has been used with niobium [23-25], iron [26], tungsten [27] and meteorite [28]. All searches using the Millikan method or the levitometer method have reported *no* evidence of fractional electric charge except for the search by LaRue *et al* [23] in niobium. But later searches in niobium using about four times as much material [24,25] found no evidence for fractional electric charge. The LaRue *et al* [23] report is not accepted today.

The largest bulk matter search using either the Millikan method or the levitometer method is our 2002 search [8,9] using about 70 mg of silicone oil. This search set a 95% confidence upper limit of 1.17 x 1022 fractionally charged particles per nucleon in the oil.

No evidence for fractionally charged particles has been found in searches using particle accelerators or colliders and no evidence has been found in searches using cosmic rays or other particles impinging on the Earth such as dark matter particles. The only reviews of these searches are the brief one in [21] and old reviews [29,30]. Examples of recent searches in colliders are the 2003 search using proton-antiproton collisions at 1800 GeV [31] and the 1998 search using electron-positron collisions at 130 GeV to 183 GeV [32]. An example of a search in particles impinging on the Earth is the 2000 search by Ambrosio *et al* [33].

8. Conclusions and discussion

While Millikan's method of determining the value of the fundamental unit of charge has been superceded by methods based on electrochemistry, Millikan's method is still used in basic science for determining the charge on small objects such as dust particles and fluid microdrops. Updated with the use of modern machine-vision technology using CCD cameras and personal computers, real-time measurements of the charge on fluid microdrops accurate to better than 1/50 of an electron charge for 7μm diameter drops, and 1/23 of an electron charge for 25μm diameter, have been taken in fractions of a second.

Since the charge-measurement accuracy of the Millikan technique is limited by Brownian motion modern implementations of Millikan systems have not significantly improved upon the charge-measurement accuracy achieved in the original system used in 1910. However, in applications such as the search for fractional electric charge where a high measurement rate is required of a Millikan apparatus, large improvements of almost eight orders of magnitude in measured mass throughput have been made. These increases in mass throughput in modern automated Millikan systems have come about from improvements associated with precision microdrop generation, machine-vision systems and power inexpensive computing which permits the real-time simultaneous charge measurements of multiple drops in the same image field and the detection and correction of measurement artifacts.

Compared with other methods for searching for fractional electric charge, the Millikan method requires by far the easiest to fabricate, least expensive hardware. As a means of searching bulk matter for fractional charge the Millikan method was until recently handicapped by a low mass throughput compared with methods utilizing magnetic levitation. This measurement rate deficiency changed in the 1990s with the availability of modern machine-vision hardware, inkjet technology and powerful low-cost networked personal computers which, after incorporation into state-of-the-art Millikan charge-measurement systems, increased mass throughput to nearly eight orders of magnitude higher than Millikan's original implementation of the experiment. Additionally, it appears possible to scale up the mass throughput several more orders of magnitude by upgrading to improved machine-vision systems and computer hardware as industry makes them available.

As final important scientific points in utilizing automated Millikan systems to search for fractional charge, the Millikan technique relies upon simple well-understood physics that enhances the credibility of the results, and in comparison with most contemporary particle physics experiments is extremely inexpensive to replicate and operate should fractional charge be detected and other institutions need to confirm the findings.

9. Acknowledgements

In addition to the authors, there were many individuals whose work and ideas went into the conception, design, and execution of the automated Millikan system experiments at SLAC. The decade-long work at the Stanford Linear Accelerator Center on automated Millikan systems for the detection of stable, fractionally charged, free particles was initiated in response to system design studies in which many of the original ideas were conceived by physicists Charles Hendricks, Gordon Shaw, Klaus Lackner, and Ed Garwin. The initial hardware designs were done aided by physicist Charles Hendricks and SLAC mechanical engineer Gerard Putallaz.

Most of the actual work in physically constructing and running the experiments was done by graduate students including Nancy Mar, George Fleming, and Brendan Casey, all of whom now have their doctorates in physics. Later work, much of it still ongoing, on the formulation of ejection-compatible fluids and the control of the electric charges of ejected microdrops was performed by post-doctoral researchers Dinesh Loomba, Sewan Fan, and SLAC associate engineer Howard Rogers. This work was supported by Department of Energy contract DE-AC03-76SF00515.

References

1. R. A. Millikan, “A new modification of the cloud method of determining the elementary electric charge and the most probable value of that charge,” *Phil. Mag.* **19** 209-28 (1910).
2. R. A. Millikan, "The isolation of an ion, a precision measurement of its charge, and the correction of Stokes' law," *Phys. Rev.* **32** 349-97 (1911).
3. P.C. Reist , *Aerosol Science and Technology*, 2nd ed., (New York: McGraw Hill) pp. 60-3 (1993).
4. W. B. Kunkel and J. W. Hansen, “A dust electricity analyzer,” *Rev. Sci. Instrum.* **21** 308-314 (1950).
5. M. Polat, H. Polat and S. Chandler, “Electrostatic charge on spray droplets of aqueous surfactant solutions,” *J. Aerosol Sci.* **31** 551-62 (2000).
6. V. D. Hopper and T. H. Laby, “The electronic charge,” *R. Soc. Lond. Ser. A* **178** 243-72 (1941).
7. D. Loomba, V. Halyo, E. R. Lee, I. T. Lee, M. L. Perl, “A new method for searching for free fractional charge particles in bulk matter,” *Rev. Sci. Instrum.* **71** 3409-14 (2000).
8. I. T Lee, S. Fan, V. Halyo, E. R. Lee, P. C. Kim, M. L. Perl, H. Rogers, D. Loomba, K. S. Lackner, G. Shaw, “Large bulk matter search for fractional charge particles,” *Phys. Rev.* D **66** 012002-1 - 012002-10 (July 1, 2002).
9. I. T Lee, Large Bulk Matter Search for Fractional Charge Particles, *Ph.D. dissertation Stanford University*, 2002.
10. W. E. Langlois, *Slow Viscous Flow*, (New York: Macmillan) 1964.
11. M. L. Savage, R. W. Bland, C. L. Hodges, J. L. Huntington, D. C. Joyce, R. T. Johnson, T. D. Knoop, M. A. Lindgren, M. H. Scholz, A. B. Steiner and B. A. Young, “A search for fractional charges in native mercury,” *Phys. Lett.* B **167** 481-4 (1986).
12. W. C. Hinds, *Aerosol Technology 2nd Ed.*, (New York: Wiley-Interscience), p. 99 (1999).
13. V. Halyo, P. Kim, E. R. Lee, I. T. Lee, D. Loomba, and M. L. Perl, “Search for free fractional electric charge elementary particles using an automated Millikan oil drop technique,” *Phys. Rev. Lett.* **84** 2576-2579 (2000).
14. V. Halyo, A Search for Free Fractional Electric Charge Elementary Particles, *Ph.D. dissertation Stanford University, SLAC Report* 565, Department of Energy, 2000.
15. N. M. Mar, E. R. Lee, G. R. Fleming, B. C. K. Casey, M. L. Perl, E. L. Garwin, C. D. Hendricks, K. S. Lackner, G. L. Shaw, “Improved search for elementary particles with fractional electric charge,” *Phys. Rev.* D **53** 6017-32 (1996).
16. N. M. Mar, A new search for elementary particles with fractional electric charge using an improved Millikan technique, *Ph.D. dissertation, Stanford University*, 1996.
17. S. L. Zoltan, (Clevite Corp.), Pulse droplet ejection system, *U.S. Patent* 3683212, 1972.

18. C. L. Hodges, P. Abrams, A. R. Baden, R. W. Bland, D. C. Joyce, J. P. Royer, F. W. Walters, E. G. Wilson, P. G. Y. Wong, and K. C. Young, "Results of a search for fractional charges on mercury drops," *Phys. Rev. Lett.* **47** 1651-3 (1981).
19. D. C. Joyce, P. C. Abrams, R. W. Bland, R. T. Johnson, M. A. Lindgren, M. H. Savage, M. H. Scholz, B. A. Young and C. L. Hodges, "Search for fractional charges in water," *Phys. Rev. Lett.* **51** 731-4 (1983).
20. P. F. Smith, "Searches for fractional electric charge in terrestrial materials," *Annu. Rev. Nucl. Part. Sci.* **39** 73-111 (1989).
21. M. L. Perl, P. C. Kim, V. Halyo, E. R. Lee, I. T. Lee, D. Loomba, and K. S. Lackner, "The search for stable, massive, elementary particles," *Int. J. Mod. Phys.* **16** 2137-64 (2001).
22. M. Marinelli and G. Morpurgo, "Searches of fractionally charged particles in matter with the magnetic levitation techniques," *Phys. Rep.* **85** 161-258 (1982).
23. G. S. LaRue, J. D. Phillips, and W. M. Fairbank, "Observation of fractional charge of (1/3)*e* on matter," *Phys. Rev. Lett.* **46** 967-70 (1981).
24. P. F. Smith, G. J. Homer, J. D. Lewin, H. E. Lewin, and W. G. Jones, "A search for fractional electric charge on levitated niobium spheres," *Phys. Lett.* B **153** 188-94 (1985).
25. P. F. Smith, G. J. Homer, J. D. Lewin, H. E. Walford, and W. G. Jones, "Searches for fractional electric charge on niobium samples exposed to liquid helium," *Phys. Lett.* B **181** 407-13 (1986).
26. M. Marinelli and G. Morpurgo, "The electric neutrality of matter: a summary," *Phys. Lett.* B **137** 439-42 (1984).
27. P. F. Smith, G. J. Homer, J. D. Lewin, H. E. Walford, and W. G. Jones, "Searches for fractional electric charge in tungsten," *Phys. Lett.* B **197** 447-51 (1986).
28. W. G. Jones, P. F. Smith, G. J. Homer, J. D. Lewin, and H. E. Walford, "Searches for fractional electric charge in meteorite samples," *Z. Phys.* C **43** 349-55 (1989).
29. L. W. Jones, "A review of quark search experiments," *Rev. Mod. Phys.* **49** 717-52 (1977).
30. L. Lyons, "Quark search experiments at accelerators and in cosmic rays," *Phys. Rep.* **129** 225-84 (1985).
31. D. Acosta, *et al.*, "Search for long-lived charged massive particles in proton-antiproton collisions at 1.8 TeV," *Phys. Rev. Lett.* **90** 131801 (2003).
32. K. Ackerstaff, *et al.*, "Search for stable and long lived massive charged particles in electron positron collisions at 130 GeV-183 GeV," *Phys. Lett.* B **433** 195-209 (1998).
33. M. Ambrosio, *et al.*, "A search for lightly ionizing particles with the MACRO detector," *Phys. Rev.* D **62** 052003 (2000).

Figure 1. Force diagram for a microdrop in a conventional Millikan apparatus. In a conventionally configured Millikan apparatus all of the forces exerted on fluid microdrops are summed in the vertical direction. The forces on a microdrop in a conventional Millikan electric charge-measurement apparatus are gravity, the electric field-induced forces, and fluid dynamic forces. The induced dipole forces can be eliminated by measuring in a uniform, gradient-free region of the electric field, where the distances between the measured microdrop and other microdrops are large. The remaining electric field force is then equal to the product of the charge on the drop and the electric field. The summed forces from gravity and the applied electric field that act to accelerate the drop are opposed by frictional fluid dynamic forces. In the Reynolds number regime that applies to micrometer dimensioned fluid microdrops in a Millikan apparatus, the fluid dynamic frictional force can be accurately described by Stokes' Law. The drops rapidly assume terminal velocity since the relaxation time constant for micrometer dimensioned microdrops is of the order of a thousandth of a second or less. By knowing the density of the microdrop fluid and the fluid dynamic properties of the gas the drop is falling in, one can, by taking terminal velocity measurements with two different values of electric field, determine the radius and the electric charge of the fluid microdrop.

Figure 2. Force diagrams for a Millikan apparatus utilizing a horizontal electric field, with optional laminar airflow to reduce the velocity of vertical fall. In a horizontal electric field Millikan apparatus the vertical terminal velocity component of a falling drop is used to extract the radius of the drops, and from these data, the horizontal terminal velocity can be used to calculate the charge on the fluid microdrop. Unlike in a Millikan apparatus with vertical electric field in which the gravitational force is in the same direction as the electric field force, in a Millikan apparatus with horizontal electric field, since gravity and the electric field forces are perpendicular to each other, the electric field does not have to assume more than one value in order for a charge measurement to be made. The horizontal electric field orientation has a much larger droplet-entrance area than that feasible with a conventional Millikan apparatus. The lack of need to switch the electric field in order to measure charge, and the large area in which droplets can be introduced into the apparatus and measured, have made this configuration preferred for the study of the properties of charged-aerosol clouds where relatively crude charge measurements on individual droplets are adequate [4,5]. For precision charge measurements on individual droplets the electric field should optimally be symmetrically switched so that droplets with different electric charges fall with the same average trajectory so that the imaging system can be set to take multiple position measurements with optimized magnification for accurate centroiding. Precisely regulated laminar airflow can be used to slow the fall velocity of large fluid microdrops in order to obtain better measurement statistics for drops with large terminal velocities.

Figure 3. Relative airflow-velocity profiles across a rectangular duct in the long (perpendicular to e-field) and short (parallel to e-field) dimensions. The airflow velocity goes to zero at the walls and increases with an approximate parabolic function towards the center of the duct. The long dimension of the duct has a plateau over which flow is relatively constant.

Figure 4. System block diagram for an automated Millikan microdrop charge-measurement apparatus. The experimental system shown in this figure operated from 1994-1995 [15,16]. Real-time image acquisition and charge measurements were implemented using a commercial-

grade monochrome CCD camera and a 66 MHz 486-based personal computer. Approximately 6 million drops were measured with an accuracy of 1/40 of an electron charge using this apparatus.

Figure 5. Mechanical layout of the automated Millikan system shown in figure 4. The measurement region between the electric field plates is convection shielded within two separate, transparent wall enclosures. The upper electric field plate is grounded and is used as a mechanical mounting surface for the microdrop ejector. The lower electric field plate is mounted on an insulated surface and is switched between precisely regulated positive and negative high voltages.

Table 1. Summary of automated machine-vision based Millikan devices constructed and operated at the Stanford Linear Accelerator Center between 1994 and 2002. Data from Robert Millikan's original experiment is listed to provide a historical reference.

Figure 1.

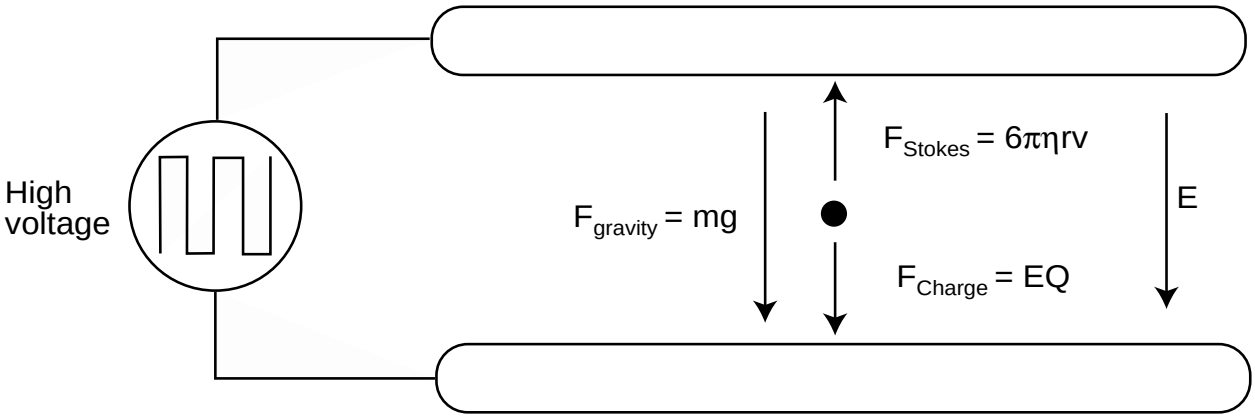

$$mg + E_{down}\, Q = 6\pi\eta r v_{down}$$

$$mg - E_{up}\, Q = 6\pi\eta r v_{up}$$

Figure 2.

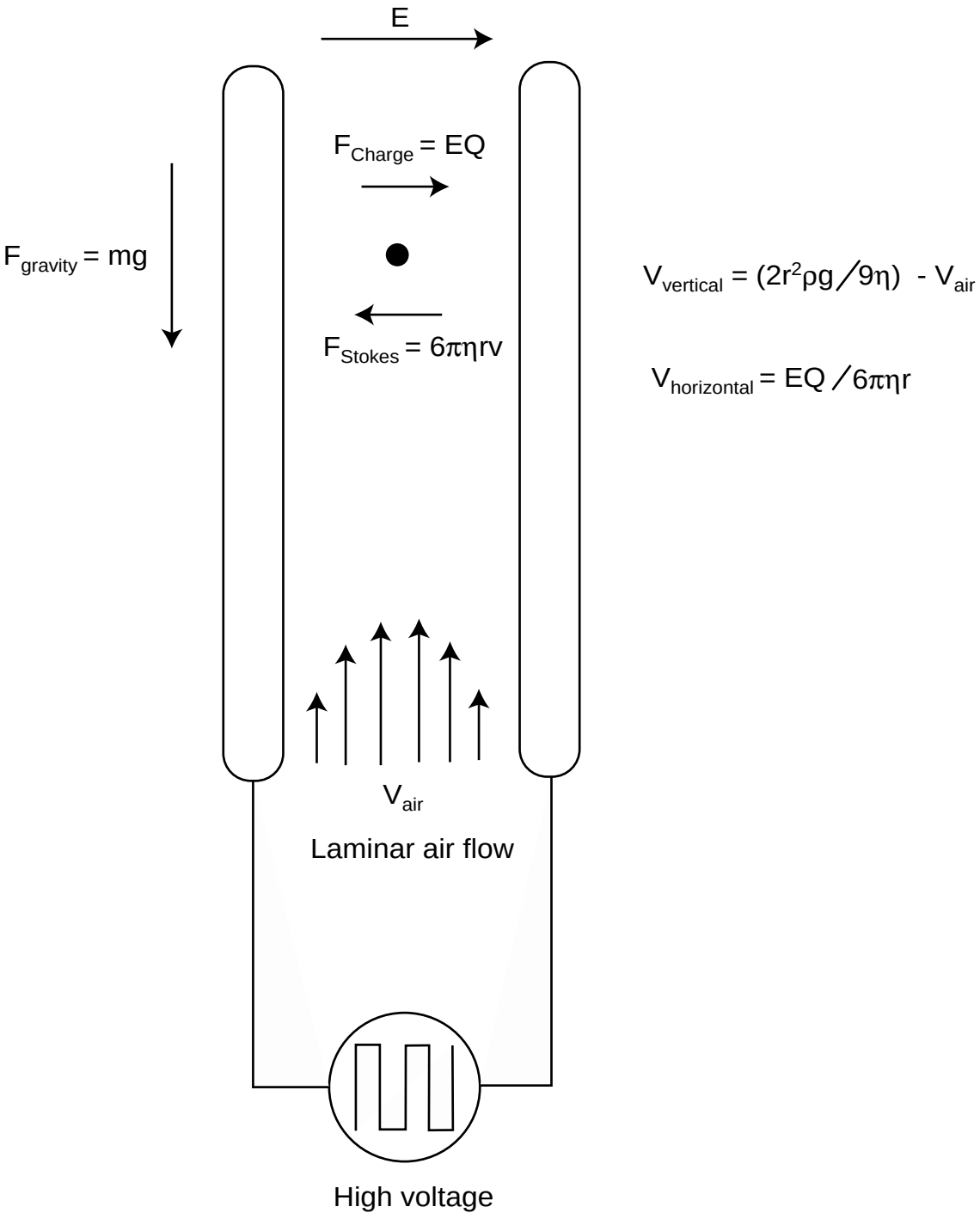
E
$F_{Charge} = EQ$
$F_{gravity} = mg$
$F_{Stokes} = 6\pi\eta rv$
$V_{vertical} = (2r^2\rho g / 9\eta) - V_{air}$
$V_{horizontal} = EQ / 6\pi\eta r$
V_{air}
Laminar air flow
High voltage

Figure 3.

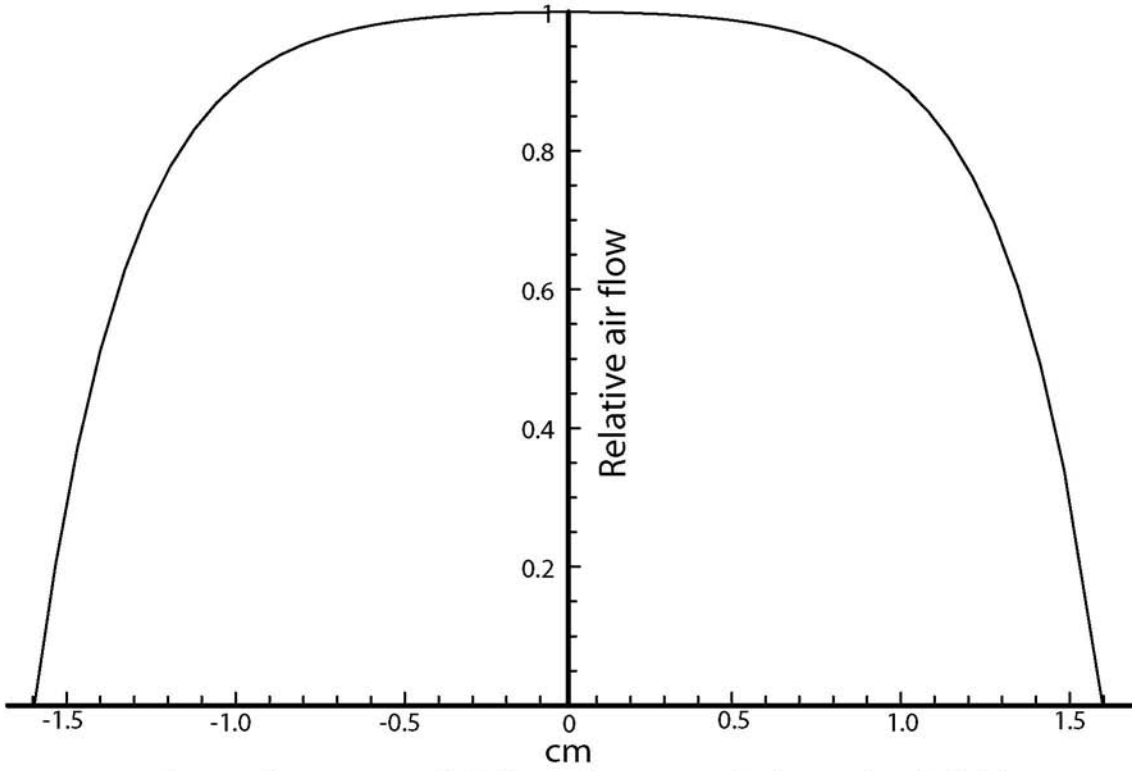
1
0.8
0.6
0.4
0.2
Relative air flow
-1.5
-1.0
-0.5
0
0.5
1.0
1.5
cm
Distance from center of air flow tube perpendicular to electric field

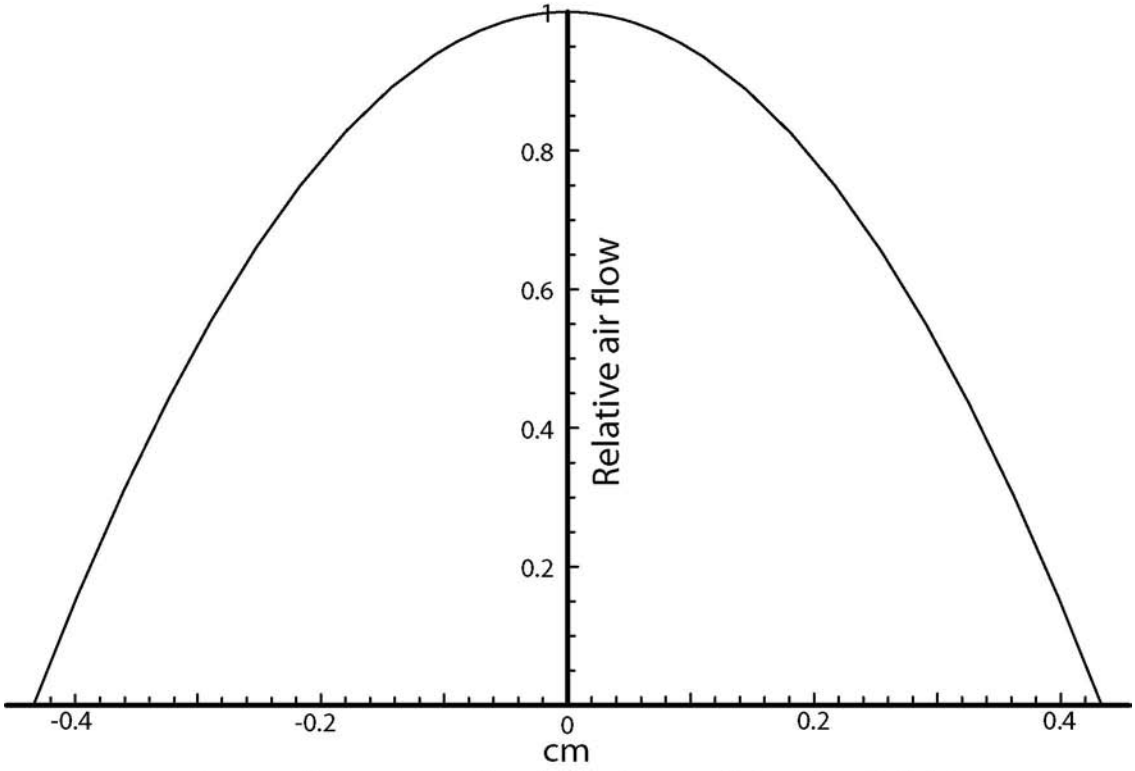
1
0.8
0.6
0.4
0.2
Relative air flow
-0.4
-0.2
0
0.2
0.4
cm
Distance from center of air flow tube parallel to electric field

Figure 4.

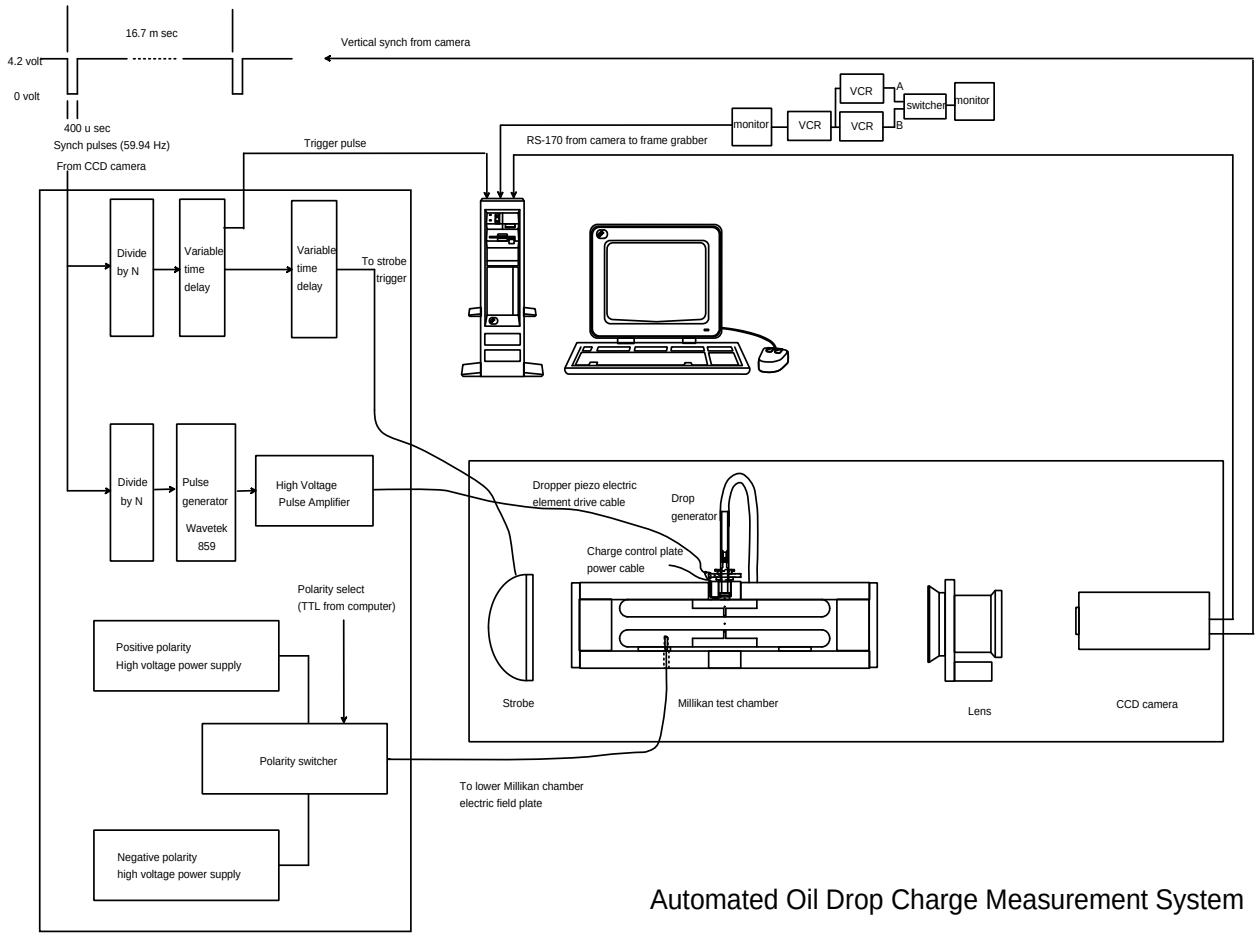

Automated Oil Drop Charge Measurement System

Figure 5.

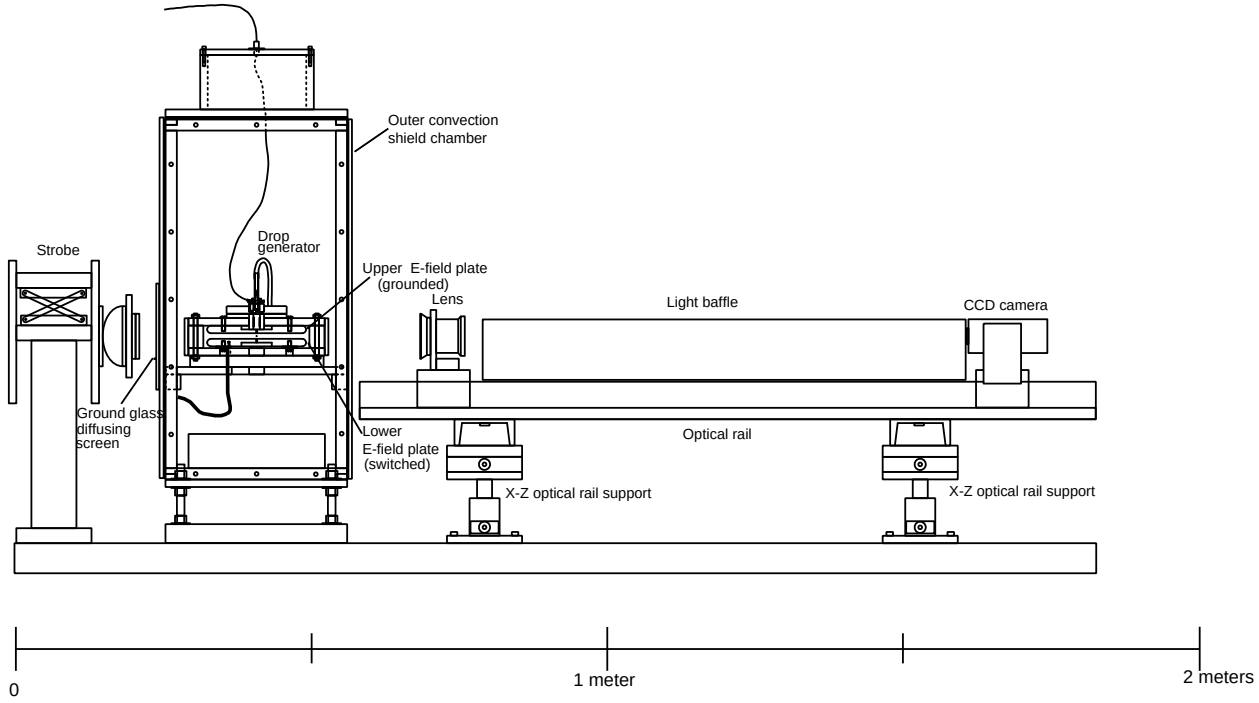
Outer convection
shield chamber
Strobe
Drop
generator
Upper E-field plate
(grounded)
Lens
Light baffle
CCD camera
Ground glass
diffusing
screen
Lower
E-field plate
(switched)
Optical rail
X-Z optical rail support
X-Z optical rail support
0
1 meter
2 meters